THE ASTROPHYSICAL JOURNAL, 474:1–12, 1997 January 1

HOW SMALL WERE THE FIRST COSMOLOGICAL OBJECTS?

MAX TEGMARK
Max-Planck-Institut für Physik, Föhringer Ring 6, D-80805 München; max@ias.edu

JOSEPH SILK
Departments of Astronomy and Physics, and Center for Particle Astrophysics, University of California, Berkeley, California 94720; silk@pac2.berkeley.edu

MARTIN J. REES
Institute of Astronomy, University of Cambridge, Cambridge CB3 OHA, UK; mjr@ast.cam.ac.uk

ALAIN BLANCHARD
Observatoire de Strasbourg, 11 rue de l'Université, 67000 Strasbourg, France; blanchard@cdsxb6.u-strasbg.fr

TOM ABEL
Max-Planck-Institut für Astrophysik, Karl-Schwarzschild-Strasse 1, D-85740 Garching; abel@mpa-garching.mpg.de

AND

FRANCESCO PALLA
Osservatorio Astrofisico di Arcetri, Largo E. Fermi, 5-50125 Firenze, Italy; palla@arcetri.astro.it
Received 1995 December 22; accepted 1996 February 29

ABSTRACT

The minimum mass that a virialized gas cloud must have in order to be able to cool in a Hubble time is computed, using a detailed treatment of the chemistry of molecular hydrogen. With a simple model for halo profiles, we reduce the problem to that of numerically integrating a system of chemical equations. The results agree well with numerically expensive three-dimensional simulations, and our approach has the advantage of being able to explore large regions of parameter space rapidly. The minimum baryonic mass M_b is found to be strongly redshift dependent, dropping from $10^6\ M_\odot$ at $z \sim 15$ to $5 \times 10^3\ M_\odot$ at $z \sim 100$ as molecular cooling becomes effective. For $z \gg 100$, M_b rises again, as cosmic microwave background photons inhibit H_2 formation through the H^- channel. Finally, for $z \gg 200$, the H_2^+ channel for H_2 formation becomes effective, driving M_b down toward $M_b \sim 10^3\ M_\odot$. With a standard cold dark matter power spectrum with $\sigma_8 = 0.7$, this implies that a fraction 10^{-3} of all baryons may have formed luminous objects by $z = 30$, which could be sufficient to reheat the universe.

Subject heading: cosmology: theory — early universe — galaxies: formation

1. INTRODUCTION

1.1. *When Did the Universe Reheat? Observational Constraints*

It is now widely accepted that the universe underwent a reheating phase at some point after the standard recombination epoch at redshift $z \approx 10^3$. However, the question of when this happened remains open. The absence of a Gunn-Peterson trough in the spectra of high-redshift quasars has provided strong evidence for the reheating occurring at a redshift $z > 5$, since it indicates that the intergalactic medium (IGM) was highly ionized at lower redshifts (Gunn & Peterson 1965; Steidel & Sargent 1987; Webb et al. 1992). The smallest baryonic objects to go nonlinear in a standard cold dark matter (CDM) model are expected to reionize the IGM at a redshift somewhere in the range $10 < z < 100$ (Bond & Szalay 1983; Couchman 1985; Couchman & Rees 1986; Fukugita & Kawasaki 1991; Tegmark, Silk, & Blanchard 1994; Tegmark & Silk 1995; Liddle & Lyth 1995). In recent models with baryonic dark matter, reheating and reionization are predicted to occur at an even higher redshift, typically in the range $100 < z < 1000$ (Peebles 1987; Gnedin & Ostriker 1992; Cen, Ostriker, & Peebles 1993).

A reheating epoch would have at least two interesting classes of effects that may be measurable today: effects on subsequent structure formation and effects on the cosmic microwave background (CMB) radiation. Subsequent structure formation would be affected in at least two ways:

1. The heating of the IGM up to a higher adiabat would raise the Jeans mass, thus suppressing the formation of small objects. For instance, an IGM temperature of 10^5K at a redshift of a few would suppress the formation of galaxies of mass below $10^{10}\ M_\odot$, thus alleviating the ubiquitous problem of theories overpredicting the abundance of faint galaxies (e.g., Blanchard, Valls-Gabaud, & Mamon 1992; Kauffman, White, & Guiderdoni 1993; Cole et al. 1994).

2. If the objects that reheat the IGM also enrich it with heavy elements, the ability of gas to cool would be greatly enhanced in the temperature range $10^4\ \mathrm{K} < T < 10^7\ \mathrm{K}$, presumably facilitating future structure formation.

The CMB would be affected in at least three ways:

1. Hot ionized IGM would cause spectral distortions that might violate the stringent limits on the Compton y-parameter (Mather et al. 1994). This is a problem mainly for baryonic dark matter (BDM) models (Tegmark & Silk 1994).

2. Spatial fluctuations on angular scales below a few degrees may be suppressed, while fluctuations on larger scales would remain fairly unaffected. Therefore, a comparison of the results of current and future degree scale experiments with those of *COBE* (Smoot et al. 1992) constrains the reionization epoch.

3. New spatial fluctuations will be generated on smaller angular scales, through the so called Vishniac effect (Vishniac 1987; Hu, Scott, & Silk 1994). The current upper

limit on CMB fluctuations on the 1′ scale (Subrahmanyan et al. 1993) places constraints on some reheating scenarios.

In other words, with the recent surge in CMB experiments and the considerable numerical, theoretical, and observational results on structure formation, the thermal history of the universe is now coming within reach of our experimental probes. In view of this, it is very timely to investigate theoretically the nature of the reheating epoch in greater detail, and to investigate the properties of the objects that caused it. In this paper we will focus on two of the most basic attributes of these first objects: their mass and their formation redshift. Hence the goal is to derive the mass-redshift distribution of the very first objects that might be able to reheat the universe, and thus set the stage for all subsequent cosmological events.

1.2. *What Does Theory Predict?*

In both CDM and BDM models of structure formation, the first objects predicted to go nonlinear are the smallest ones. The crucial question is whether cooling will allow the baryonic clouds to dissipate their kinetic energy and collapse more than the dark matter, to eventually become self-gravitating and form an interesting object such as a galaxy, a very massive object (VMO), or a black hole (see, e.g., Binney 1977; Rees & Ostriker 1977; Silk 1977; White & Rees 1978; Araujo & Opher 1988, 1989, 1991). For low-mass objects, the smaller they are, the less efficiently they dissipate energy and cool. Thus a detailed treatment of gas-dynamical processes will predict a characteristic mass scale M_c such that objects with $M > M_c$ can cool rapidly, whereas smaller lumps will merely remain pressure-supported and not form anything luminous. In other words, M_c is the mass scale of the first luminous objects.

Fortunately, making a theoretical estimate of M_c is much simpler than the corresponding problem for present-day structure formation. Today there are large uncertainties both in the metal abundance of the IGM, which affects cooling rates, and in the UV background, which affects ionization rates and molecular chemistry. Before the first structures formed, there were by definition neither metals nor UV background.

The problem has recently been treated realistically using a multifluid three-dimensional cosmological hydrodynamics code which not only evolves the dark and baryonic matter but also tracks the nonequilibrium chemistry of nine species, including hydrogen molecules (Abel 1995; Anninas et al. 1996; Abel et al. 1996a). The main obstacle to this program is computational expense, because of the large dynamical range involved. As a complement to such heavy computations, it is thus worthwhile to attack the problem with various approximate techniques that are fast enough to run many times, thereby exploring all of parameter space and finding out which parameter choices and initial conditions merit more detailed numerical studies. This is the purpose of the present paper. One such approximate method is that of Haiman, Thoul, & Loeb (1996b, hereafter HTL96), which numerically follows the growth of an isolated density peak that is spherically symmetric. Although the first structures to collapse in CDM are typically sheet-like rather than spherically symmetric, this model nonetheless illustrates which physical processes are likely to be the most important in the full three-dimensional case. Since the approach of HTL96 involves numerically integrating a partial differential equation (separately tracking a large number of spherical shells), it is still fairly time-consuming, and results are presented for only 24 points in the M-z plane (see Fig. 6 below). In this paper, we use a still simpler approach, involving nothing but ordinary differential equations, which turns out to reproduce the results of HTL96 quite well. The resulting code is so fast that we can run it thousands of times, thereby finding the curve in Figure 6 below that delimits collapsing objects from noncollapsing ones, and study the way in which this curve depends on cosmological parameters such as Ω, Ω_b, and h.

For the various CDM-based scenarios, the first interesting objects will turn out to be rare peaks in the Gaussian random field of mass between 10^4 and 10^7 $M_\odot$, at redshifts in the range $20 \lesssim z \lesssim 100$. At these redshifts, the initial IGM temperature is considerably lower than the virial temperatures in question, so the baryons will initially collapse together with the dark matter. These first objects will have virial temperatures between a few hundred and a few thousand degrees, which means that the main coolant will be molecular hydrogen. (Line cooling by hydrogen and helium is negligible for $T \ll 10^4$ K, and lithium hydride and other less abundant molecules become dominant only when $T \ll 500$ K.) In § 2, accurate expressions for H_2 cooling are presented, and it is shown that the precollapse H_2 abundance is typically too low for the clouds to cool significantly in a Hubble time. The fate of a virialized lump thus depends crucially on its ability to rapidly produce more H_2, which is the topic of § 3. Our simple model for the evolution of density and temperature is presented in § 4, and the numerical results are described in § 5. The results and their cosmological implications are discussed in § 6.

2. COOLING BY MOLECULAR HYDROGEN

How much molecular hydrogen is needed for a gas cloud to be able to cool in a Hubble time? This question will be answered in the present section. The atomic physics of molecular hydrogen cooling has been studied extensively by many authors, e.g., Lepp & Shull (1983). An excellent review of what will be needed here is given by Hollenbach & McKee (1979, hereafter HM), who also provide a number of useful analytical fits to various numerical results.

When an H_2 molecule is rotationally or vibrationally excited through a collision with an H atom or another H_2 molecule, there are two competing channels through which the ensuing de-excitation can occur. Either the de-excitation is radiative, which amounts to cooling, or it is collisional, in which case there is no net energy loss from the gas. When the density n is very low, the former channel dominates. In this case, the hydrogen molecules spend most of their time in the ground state or in the $J = 1$ rotational state (whose radiative decay to the ground state is forbidden, since H_2 has no dipole moment), and collisional excitations are for all practical purposes instantly followed by a radiative decay. Thus in the low-density limit, the energy loss per unit volume is proportional to n^2. When the density n is very high, on the other hand, collisions dominate. Thus, to a good approximation, the distribution of molecules in various states is the Boltzmann distribution of local thermal equilibrium (LTE), and the energy loss per unit volume is only linear in n. The border between "high" and "low" density is roughly the function $n_{\rm cr}$ defined below. It is temperature dependent, but lies between 10^3 and 10^4 cm^{-3} for our regime of interest, 10^2 K $< T < 10^3$ K. A just virialized

gas cloud has an overdensity of about $18\pi^2 \approx 178$, i.e., a hydrogen density

$$n \approx 23 \text{ cm}^{-3}\left(\frac{h^2\Omega_b}{0.015}\right)z_{100}^3 , \quad (1)$$

so during the early stages of collapse, we are well into the low-density regime for our parameter range of interest. (Here and throughout this paper we assume a helium abundance of 24% by mass.)

Since the fraction f of hydrogen in molecular form will be quite low in our application (typically below 10^{-3}), we can neglect H_2-H_2 collisions, and the formulae of HM reduce to the following: The cooling rate is

$$L \approx \frac{L_r^{(\text{LTE})}}{1 + n_{\text{cr}}/n} , \quad (2)$$

where the critical density is

$$n_{\text{cr}} \equiv \frac{L_r^{(\text{LTE})}}{L_r^{(n\to 0)}}\, n , \quad (3)$$

which depends only on temperature, not on n. Here the cooling rate in LTE is

$$L_r^{(\text{LTE})} \approx \frac{1}{n}\left\{\left(\frac{9.5\times 10^{-22}T_3^{3.76}}{1 + 0.12T_3^{2.1}}\right)e^{-(0.13/T_3)^3} + 3\times 10^{-24}e^{-0.51/T_3}\right\} \text{ ergs cm}^3 \text{ s}^{-1} , \quad (4)$$

whereas the cooling rate in the low-density limit is

$$L_r^{(n\to 0)} \approx \tfrac{5}{4}\gamma_2(E_2 - E_0)e^{-(E_2-E_0/kT} + \tfrac{7}{4}\gamma_3(E_3 - E_1)e^{-(E_3-E_1)/kT} . \quad (5)$$

Here $T_3 = T/1000$ K, $E_J = J(J+1)E_1/2$, where $E_1/k \approx 171$ K. Thus $(E_2 - E_0)/k = (3/5)(E_3 - E_1)/k = 3E_1/k \approx 512$ K. The parameters γ_2 and γ_3 are the collisional de-excitation rates from the $J = 2$ and $J = 3$ rotational levels. The rates for collisional quadrupole de-excitation $J \to J - 2$ due to the impact of hydrogen atoms are well fitted by (HM)

$$\gamma_J(T) = \left(\frac{10^{-11}T_3^{1/2}}{1 + 60T_3^{-4}} + 10^{-12}T_3\right) \times \left\{0.33 + 0.9\exp\left[-\left(\frac{J-3.5}{0.9}\right)^2\right]\right\} \text{ cm}^3 \text{ s}^{-1} . \quad (6)$$

Equation (5) assumes an ortho-H_2 to para-H_2 ratio of 3:1. The first term gives the cooling contribution of para-H_2, and the second that of ortho-H_2. Abel et al. (1996b) show that for H_2 formation by the gas-phase reactions discussed in the following section, the interconversion mechanism,

$$H_2(\text{ortho}) + H^+ \to H_2(\text{para}) + H^+ , \quad (7)$$

will be fast enough to convert all ortho-H_2 to para-H_2. Hence the appropriate cooling rate is given by the first term in equation (5) multiplied by 4, i.e., equation (5) is replaced by simply

$$L_r^{(n\to 0)} \approx 5\gamma_2(E_2 - E_0)e^{-(E_2-E_0)/kT} . \quad (8)$$

Defining the *cooling timescale* $\tau_{\text{cool}} \equiv T/\dot{T}$, we thus obtain

$$\tau_{\text{cool}} \approx 48{,}200 \text{ yr}\left(1 + \frac{10T_3^{7/2}}{60 + T_3^4}\right)^{-1} e^{512\text{ K}/T}(fn_1)^{-1} , \quad (9)$$

where $n_1 \equiv n/1 \text{ cm}^{-3}$. Let us define the *Hubble timescale* τ_{H} at a redshift z as the age of the universe at that redshift. Then, for $\Omega = 1$,

$$\tau_{\text{H}} \approx 6.5\times 10^6 \text{ yr } h^{-1}z_{100}^{-3/2} . \quad (10)$$

Since the primordial gas clouds in which we are interested have just virialized, the Hubble timescale is of the same order as the *gravitational timescale*, $\tau_g \equiv (\rho G)^{-1/2}$, the timescale on which collapse would proceed if the temperature were lowered and the clouds lost their pressure support. Thus the future of a newly formed gas cloud is crucially dependent on the ratio $\tau_{\text{cool}}/\tau_{\text{H}}$ (Rees & Ostriker 1977). If $\tau_{\text{cool}} \ll \tau_{\text{H}}$, the gas cloud will rapidly cool and begin a nearly free-fall collapse, whereas if $\tau_{\text{cool}} \gg \tau_{\text{H}}$, the cloud will remain pressure supported and fairly stationary until much lower redshifts. The timescale $\tau_{\text{cool}} = \tau_{\text{H}}$ for

$$f \approx 0.00016\left(\frac{h\Omega_b}{0.03}\right)^{-1} z_{100}^{-3/2}\left(1 + \frac{10T_3^{7/2}}{60 + T_3^4}\right)^{-1} e^{512\text{K}/T} . \quad (11)$$

This critical H_2 fraction is plotted in Figure 1, as a function of temperature. It is seen that the H_2 fraction required exceeds typical initial abundances ($\sim 10^{-4}$) for all redshifts $z < 200$ when $T < 10^4$ K. Thus our low-mass, high-redshift clouds can cool and collapse only if additional H_2 is produced (unless $T \gtrsim 10^4$ K, in which case hydrogen line cooling will be effective).

In the following section we will compute how much additional H_2 will be produced, and discuss the conditions that determine when sufficient cooling will indeed occur.

3. PRODUCTION OF MOLECULAR HYDROGEN

How much molecular hydrogen will be produced in a Hubble time? In hydrogen of density $n = n[\text{H}] + n[\text{H}^+] + 2n[\text{H}_2]$ at temperature $T \lesssim 10^3$ K, the ionization fraction $x \equiv n[\text{H}^+]/n$ and the molecular fraction $f \equiv n[\text{H}_2]/n$ evolve as

$$\dot{x} = -k_1 nx^2 , \quad (12)$$

$$\dot{f} = k_m n(1 - x - 2f)x . \quad (13)$$

Collisional ionization of H atoms as well as collisional dissociation of H_2 is completely negligible at such low temperatures. At the low densities in question, H_2 is formed mainly via the reaction $H + e^- \to H^- + h\nu$ at the rate k_2, after which one of the following two things happens to the H^- almost instantaneously:

1. Molecular hydrogen is produced through the reaction $H + H^- \to H_2 + e^-$, at the rate k_3.
2. The H^- gets destroyed by a CMB photon, at the rate k_4.

Thus the effective rate of H_2 formation is $k_2k_3/[k_3 + k_4/(1 - x)n]$. Since $T_\gamma \propto 1 + z$, the exponential term in k_4 effectively makes H_2 production through the H^- channel impossible for $z \gg 200$. A second, less effective channel for molecule formation is the slow reaction $H^+ + H \to H_2^+ + h\nu$ at the rate k_5, followed almost immediately by either $H_2^+ + H \to H_2 + H^+$ at the rate k_6 or photodissociation at the rate k_7, thus producing H_2 at the net rate $k_5k_6/[k_6 + k_7/(1 - x)n]$. This channel works up to higher redshifts, but since $k_5 \ll k_2$, it becomes important only for lumps with virialization redshifts $z_{\text{vir}} \gg 100$. In our calcu-

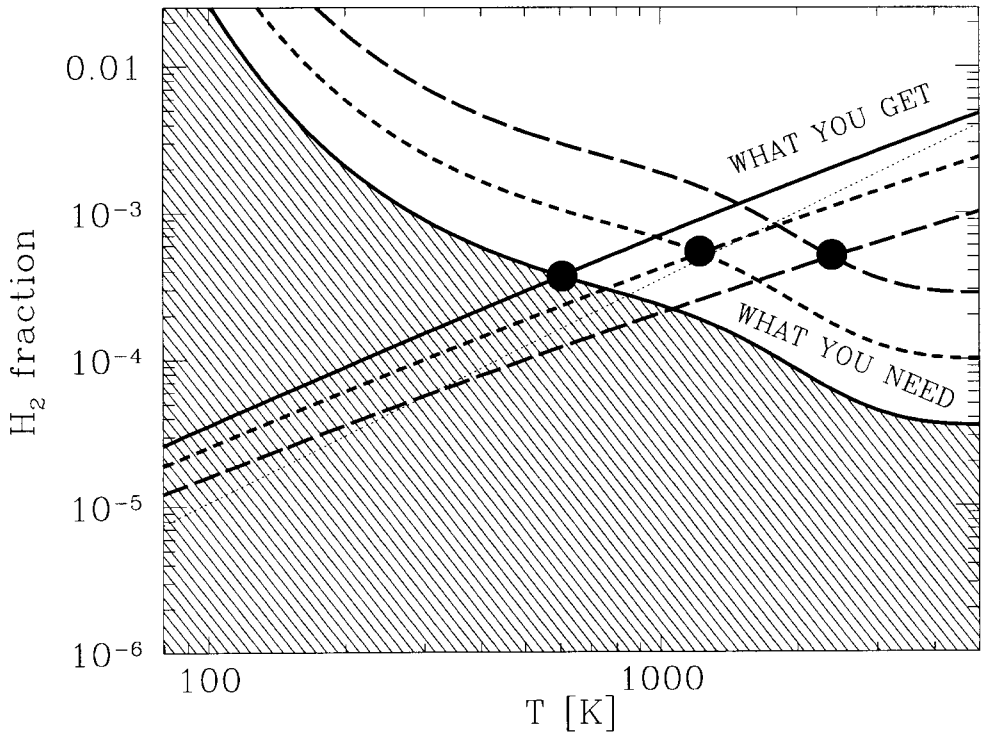

FIG. 1.—Molecular fraction needed and molecular fraction produced. The solid, short-dashed, and long-dashed lines correspond to lumps virializing at $z_{vir} = 100$, 50, and 25, respectively. Only clouds above the downward sloping lines (outside the shaded region for $z_{vir} = 100$) can cool in a Hubble time. The upward-sloping lines show the molecular fraction produced in a local Hubble time, so the minimum temperature needed for collapse is that where the pair of curves cross (*solid dots*; — lower z_{vir} require higher virial temperature). Electron depletion is the limiting factor above the thin dotted line, so we see that for $z \gtrsim 50$ the results are rather independent of the initial ionization fraction.

lations further on, we use the exact rate, i.e.,

$$k_m = \left[\frac{k_3}{k_3 + k_4/(1-x)n}\right]k_2 + \left[\frac{k_6}{k_6 + k_7/(1-x)n}\right]k_5 . \quad (14)$$

Although we integrate the above-mentioned chemical equations numerically in our analysis, a number of the features of the solutions can be readily understood from the following elementary observations. First note that equation (12) is independent of f, since the electrons act only as a catalyst in the reactions that produce H_2. Since the right-hand side of equation (12) is not linear but quadratic in x, the residual ionization fraction decays much slower than exponentially. In the absence of cooling, T and n will remain roughly constant in the pressure-supported cloud, and the solution will be

$$x(t) = \frac{x_0}{1 + x_0 n k_1 t} , \quad (15)$$

i.e., $x \to 0$ only as $1/t$, where k_1 is the recombination rate.[1] Substituting this into equation (13), we see that $f \to 1$ as $t \to \infty$, i.e., all hydrogen would become molecular if we waited long enough. With parameters in our range of interest, however, f will remain much less than unity for many Hubble times. Thus taking $1 - x - 2f \approx 1$, equation (13) has the solution

$$f(t) = f_0 + \frac{k_m}{k_1}\ln(1 + x_0 n k_1 t) \quad (16)$$

[1] To obtain better accuracy when $z \sim 10^3$, we use the more complicated rate equations given in Peebles (1993, § 6) in place of the rate k_1 from Table 1 in our numerical runs.

when k_m is roughly constant (it will be roughly constant except at $z \sim 300$ and $z \sim 100$, which is when the two radiative dissociation processes go from being dominant to being negligible). Thus the time evolution separates into two distinct regimes: $x_0 n k_1 t \ll 1$ and $x_0 n k_1 t \gg 1$. In the first regime, the residual ionization remains roughly constant, and molecules get produced at a constant rate. In the second regime, electron depletion becomes a serious problem, and the molecular fraction grows only logarithmically with time. Since the factor $1/(x_0 nk)$ is simply the recombination timescale, we can rephrase this result as stating that the molecule fraction produced is $f - f_0 = (k_m/k_1)\ln(1 + N_{rec})$, where N_{rec} is the number of recombination times elapsed. The transition occurs after about one recombination time ($N_{rec} \approx 1$), i.e., when

$$f \approx f_c \equiv \frac{k_m}{k_1} \approx 3.5 \times 10^{-4} T_3^{1.52} \times [1 + 7.4 \times 10^8 n_1^{-1}(1+z)^{2.13} e^{-3173/(1+z)}]^{-1} \quad (17)$$

for $z \ll 300$, a value that is independent of the initial ionization fraction x_0. The factor in square brackets corresponds to photodissociation of H^-, and can be ignored for $z \lesssim 100$. Figure 1 shows $f(\tau_h)$ as a function of T for $x_0 = 3 \times 10^{-4}$, together with $f_c(T)$. As can be seen, we typically have $f(\tau_h) > f_c$ for $z_{vir} \gg 50$, i.e., we are well into the electron depletion regime, which means that the final molecule abundance f is rather insensitive to the initial ionized fraction x_0 and approximately given by equation (17).

Figure 1 also shows that the three solid dots almost line up horizontally. In other words, the molecular fraction in clouds that just barely manage to collapse (where the molecular hydrogen fraction produced within a Hubble

time is just enough to make it cool in a Hubble time) is almost independent of the virialization redshift for $25 \lesssim z_{\rm vir} \lesssim 100$. Since the virial temperature of a collapsing cloud is determined only by its mass and its virialization redshift, this implies that any cloud with a molecular hydrogen fraction $\sim 5 \times 10^{-4}$ is able to cool within a Hubble time. We can summarize this with the following useful rule of thumb: If the virial temperature is high enough to produce a molecular hydrogen fraction of order 5×10^{-4}, then the cloud will collapse. This explains the rather constant slope in Figures 5 and 6 for $20 \lesssim z_{\rm vir} \lesssim 80$.

4. EVOLUTION OF DENSITY AND TEMPERATURE

In this section, we describe our simple model for how the gas density and temperature evolve in an overdensity that grows, goes nonlinear and virializes. Section 4.1 refers mainly to the dark matter; the late stages of the density evolution of the baryons are discussed in §§ 4.2 and 4.3.

4.1. *The Density*

Early on, while $z \gg \Omega_0^{-1}$, space is approximately flat and the Friedmann equation has the approximate solution

$$a(t) \propto t^{2/3} \tag{18}$$

regardless of the values of Ω_0 and the cosmological constant λ_0. If an $\Omega = 1$ universe has a completely uniform density ρ except for a "top-hat" overdensity, a spherical region where the density is some constant $\rho' > \rho$, then this top-hat region will gradually begin to expand slower than the rest of the universe, stop expanding and recollapse to a point. By Birkhoff's theorem, the radius of this region will evolve according to the Friedmann equation, but with some $\Omega > 1$. It is well known that the overdensity

$$\delta \equiv \frac{\rho'}{\rho} - 1 \tag{19}$$

evolves as

$$(1 + \delta) = \frac{9}{2} \frac{(\alpha - \sin \alpha)^2}{(1 - \cos \alpha)^3} = 1 + \frac{3}{20} \alpha^2 + O(\alpha^3) , \tag{20}$$

where the parameter α, the "development angle," is related to the redshift through

$$\frac{1 + z_{\rm vir}}{1 + z} = \left(\frac{\alpha - \sin \alpha}{2\pi} \right)^{2/3} = \frac{\alpha^2}{(12\pi)^{2/3}} + O(\alpha^{8/3}) . \tag{21}$$

Here $z_{\rm vir}$ is the redshift at which the top hat would collapse to a point. In reality, an overdense region would of course not collapse to a point (and form a black hole). Since it would not be perfectly spherically symmetric, collisionless dark matter particles would mostly miss each other as they whizzed past the central region and out again on the other side, eventually settling down in some (quasi-)equilibrium configuration known as the virial state. For baryons, gasdynamical processes become important, and pressure eventually halts the collapse at some density ρ_p as discussed in § 4.3 below. Strictly speaking, virial states are not stable over extremely long periods of time, and their density is certainly not uniform. For a virialized lump, often referred to as a "halo," a typical density profile peaks around some constant value in its core and falls off as r^{-2} over some range of radii. Nonetheless, halos are often said to have a "typical" density

$$\rho_{\rm vir} \approx 18\pi^2 \rho_0 (1 + z_{\rm vir})^3 , \tag{22}$$

which is a useful rule of thumb. Thus in the top-hat collapse model, density in the perturbed region is assumed to evolve as in Figure 2: the density starts out decreasing almost as fast as the background density ρ, with

$$\delta \propto (1 + z)^{-1}$$

early on, just as in linear theory, but gradually stops decreasing and increases radically as z approaches $z_{\rm vir}$. It never increases past the virial value $\rho_{\rm vir}$ or the pressure-determined value ρ_p, whichever is smaller, but stays at that density for all $z < z_{\rm vir}$. The main motivation for the use of the Lagrangian code in HTL96 was to provide a more realistic modeling of the spatial structure of the halo. We use the simple top-hat approximation instead, for the following reasons:

1. It requires much less computer time.
2. It reproduces the results of HTL96 fairly well.
3. The spherical symmetry assumption of HTL96 is probably somewhat inaccurate anyway, since n-body simulations have demonstrated that the first collapsed structures tend to be sheetlike pancakes rather than spherically symmetric.

In defense of the spherical symmetry assumption, very rare peaks in a random field (which might correspond to the very first objects) are typically almost spherically symmetric (Bardeen et al. 1986). More important, since the virial temperatures in our application are typically only slightly higher than the precollapse gas temperatures, none of our conclusions should be very sensitive to the actual way in which the cloud gets to its virial configuration, such as whether it first passes through an intermediate pancake-like configuration or not.

Unfortunately, α cannot be eliminated from the equations that relate δ and z by using elementary functions. For this reason, we use the following fit to the density evolution $\rho(z) = \rho_0[1 + \delta(z)]$, which is accurate to about 5% until z is within 10% of $z_{\rm vir}$ (Tegmark 1994), at which the density is assumed to start approaching the limiting value $\rho_{\rm vir}$ or ρ_p anyway:

$$\rho(z) \approx \rho_0 (1 + z)^3 \exp\left(- \frac{1.9A}{1 - 0.75A^2} \right) , \tag{23}$$

where

$$A(z) \equiv \frac{1 + z_{\rm vir}}{1 + z} , \tag{24}$$

and ρ_0 is the mean density of the universe today. We use this fit in our numerical analysis, but never let the density exceed the virial value, as shown in Figure 2.

4.2. *The Temperature*

The thermal evolution of the gas is dominated by the following processes:

1. Hydrogen line cooling (as given by eq. [26]).
2. Cooling by molecular hydrogen (as given by eq. [9]).

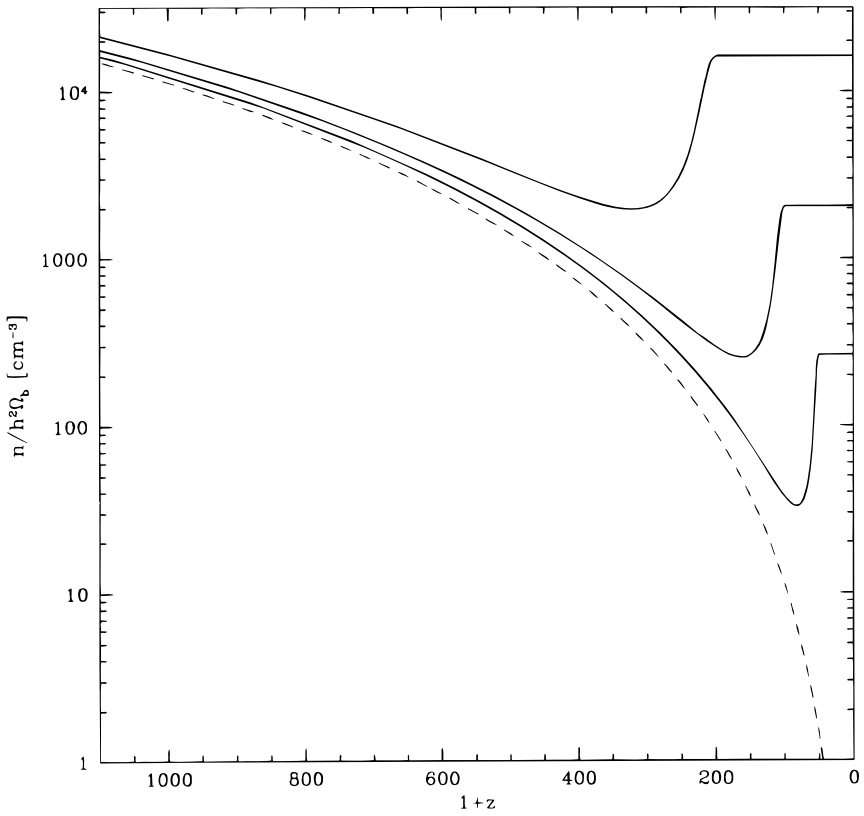

FIG. 2.—Model for density evolution. Our model for the evolution of the baryon number density $n(z)$ is shown for models with three different virialization redshifts z_{vir}, for the case of negligible pressure; n first decreases slower than the background density (*dashed line*) according to linear theory, then increases again as the lump collapses and virializes, and finally reaches the virial plateau value of $18\pi^2$ times the background density when $z = z_{vir}$.

3. Compton cooling (as given by eq. [25]).
4. Adiabatic cooling/heating (caused by the expansion/compression of the gas).

Bremsstrahlung and helium line cooling are completely negligible at the low temperatures in which we are interested. The first three mechanisms simply couple the gas atoms to the radiation field, which means that they will cause cooling when the gas is hotter than the CMB and heating otherwise. In other words, none of these mechanisms can make the gas cooler than the CMB temperature, which at $z = 100$ is a few hundred kelvins.[2] In the Compton case, this is reflected by the fact that the cooling rate is of the form

$$\left(\frac{dT}{dt}\right)_{\rm comp} = k_8\, x(T_\gamma - T)\,. \tag{25}$$

For line cooling, given by (Dalgarno & McCray 1972),

$$\Lambda_l \approx 7.5 \times 10^{-19}\ \text{ergs cm}^3\ \text{s}^{-1} e^{-118{,}348\ \text{K}/T} n^2 x(1-x)\,, \tag{26}$$

the CMB temperature is completely irrelevant, since line cooling only becomes important when $T \gg 10^3$ K, i.e., when $T \gg T_\gamma$. For the molecular case, this is included by replacing $\Lambda_m(T)$ by the net cooling rate $\Lambda_m(T) - \Lambda_m(T_\gamma)$.

The adiabatic contribution is given by the $p\,dV$ work done as the gas expands or contracts. In the simple top-hat model of the previous section, the density of the lump remains almost uniform until close to the virialization redshift z_{vir}, so that the adiabatic cooling term is simply

$$\left(\frac{dT}{dt}\right)_{\rm adiab} = \frac{2}{3}\frac{\dot{n}}{n}\,T\,, \tag{27}$$

where the baryon number density $n \propto \rho$ is given by equation (23). (The molecular abundances are so small that to a good approximation we can treat the IGM as a $\gamma = 5/3$ monatomic ideal gas.) As $z \to z_{vir}$, equation (23) would imply that $T \to \infty$, as the lump collapses to a point. Instead, the lump is assumed to settle into an approximately pressure-supported configuration, where a typical gas element will obtain the virial temperature T_{vir}. For an overdense lump of total (baryonic and dark) mass M that stops expanding, recollapses, and virializes at redshift z_{vir}, this temperature T_{vir}, which corresponds to the gas particles having velocities similar to those of the dark matter particles, is approximately (Blanchard et al. 1992)

$$T_{vir} = 485\ \text{K}\ h^{2/3}\left(\frac{M}{10^4\ M_\odot}\right)^{2/3}\left(\frac{1+z_{vir}}{100}\right). \tag{28}$$

4.3. *The Effect of Gas Pressure*

How high will the typical gas density be in this pressure-supported state? At redshifts $\gg 100$, the Compton coupling to the CMB via the small fraction (10^{-5} to 10^{-3}) of the electrons that remain ionized is still so strong that the IGM temperature will be close to that of the CMB,

$$T_\gamma \approx 273\ \text{K}\left(\frac{1+z_{vir}}{100}\right). \tag{29}$$

[2] Assuming nucleosynthesis abundances, cooling by lithium hydride is negligible compared to H_2 cooling unless $T \ll 100$ K (Puy et al. 1993; Puy & Signore 1996), so we can safely neglect lithium chemistry for our application.

As time progresses, the Compton coupling weakens, and the IGM begins to cool below the temperature T_γ, cooling adiabatically as $(1+z)^2$. Comparing equation (28) and equation (29), we therefore see that as long as $M \gg 10^4\, M_\odot$, the baryons in the ambient IGM will have a temperature considerably below $T_{\rm vir}$, and begin to fall into a virial configuration together with the cold dark matter. However, the gas density can only rise by the large factor $18\pi^2$ without problems with pressure support if $T \ll T_{\rm vir}$ *after* the collapse. Since $T \propto n^{2/3}$ during the adiabatic compression, this means that we must have $T_{\rm vir} \gg (18\pi^2)^{2/3} T \sim 32T$ before the collapse to be able to ignore pressure, and this turns out to be a good approximation for the critical masses only when $z_{\rm vir} \ll 100$. Otherwise, the condition that $T = T_{\rm vir}$ after the collapse gives only a collapse factor of order $(T_{\rm vir}/T_1)^{3/2}$, where T_1 denotes the temperature of the uniform background medium at redshift $z = z_{\rm vir}$. In other words, equation (22) is replaced by

$$\rho_p \approx \rho_0 (1+z_{\rm vir})^3 \left(\frac{T_{\rm vir}}{T_1}\right)^{3/2} . \tag{30}$$

We can obtain a more rigorous estimate of the final density as follows (Loeb 1996): Hydrostatic equilibrium after the collapse implies that gravity is balanced by pressure gradients, i.e., that the gravitational potential ϕ and the pressure p are related by

$$\nabla\phi = -\frac{1}{\rho}\nabla p . \tag{31}$$

Integrating this equation along some curve from very far outside the lump (where $\phi = 0$ by definition) to a typical point inside the lump, we thus obtain

$$\phi = \int \nabla\phi \cdot d\boldsymbol{r} = \int \frac{\nabla p}{\rho} \cdot d\boldsymbol{r} . \tag{32}$$

Since the gas has been compressed adiabatically during the collapse to this state, its pressure and density are related by

$$\left(\frac{p}{p_1}\right) = \left(\frac{\rho}{\rho_1}\right)^{5/3} , \tag{33}$$

where p_1 and ρ_1 denote the pressure and density of the uniform background medium at redshift $z = z_{\rm vir}$. Substituting this into equation (32), we obtain

$$\phi = \frac{5}{2}\frac{p_1}{\rho_1}\int \nabla\left(\frac{p}{p_1}\right)^{2/5} \cdot d\boldsymbol{r} = -\frac{5}{2}\frac{p_1}{\rho_1}\left[\left(\frac{p}{p_1}\right)^{2/5} - 1\right] . \tag{34}$$

By the ideal gas law, $p_1/\rho_1 = kT_1/m_p$, where m_p is the molecular weight. Eliminating (p/p_1) using equation (33) and defining $T_{\rm vir}$ by

$$\tfrac{3}{2}kT_{\rm vir} = -\tfrac{1}{2}m_p\phi , \tag{35}$$

we thus find the final overdensity inside the lump to be

$$(1+\delta) = \frac{\rho}{\rho_1} = \left(1 + \frac{6}{5}\frac{T_{\rm vir}}{T_1}\right)^{3/2} , \tag{36}$$

in good agreement with $(1+\delta) = (T_{\rm vir}/T_1)^{3/2}$ from equation (30) considering that the factor $\frac{1}{2}$ in the definition of $T_{\rm vir}$ in equation (35) was somewhat arbitrary. In reality, the gas evolution might not be completely adiabatic during the collapse, because of the above-mentioned cooling processes.[3] We therefore adopt the following procedure in our simulations: the gas density is evolved according to the top-hat solution until T reaches $T_{\rm vir}$. At this point, gas pressure is assumed to halt the collapse, and the gas density is held constant for the rest of the run. If the gas overdensity reaches the virial value $18\pi^2$ before T reaches $T_{\rm vir}$, then the density is held constant at this value, and the temperature is raised to $T_{\rm vir}$ (by assumed shocks).

What happens now, after $z_{\rm vir}$? If the gas is going to be able to collapse further and eventually form something like Population III stars, the baryons must now be able to dissipate energy rapidly through cooling. If this is the case, the gas cloud may get dense enough to become self-gravitating, which adds further instability to the system and may eventually lead to the formation of an extremely nonlinear object like a galaxy. The key question is thus how fast the gas in the lump can cool after $z_{\rm vir}$. This is the topic of the next section.

5. NUMERICAL RESULTS

After a lump virializes, one of two things will happen to it:

1. Enough H_2 is produced that it will enter a phase of runaway cooling and collapse.
2. Cooling will be so slow that it will remain pressure supported for a Hubble time.

In the former case, we will say that the lump *collapses*, in the latter case that it *fails* to collapse. If it fails, it will not produce any luminous objects that can reheat the IGM but will merely remain as an object resembling a small Lyman-alpha cloud. Whether a lump succeeds or fails to collapse of course depends on cosmological parameters such as h, Ω, and Ω_b. First and foremost, it depends strongly on the parameters M and $z_{\rm vir}$. In this section we first give an operational definition of what we mean by collapse, and then evolve a large number of lumps numerically to see for which parts of parameter space they manage to collapse, summarized in Figures 5 and 6.

The results of two sample runs are shown in Figures 3 and 4. Both have $T_{\rm vir} = 1000$ K and the standard CDM parameters $\Omega = 1$, $\Omega_b = 0.06$, $h = 0.5$. In Figure 3 (with $z_{\rm vir} = 100$), collapse succeeds by our criterion below. To the left, we see how recombination reduces the ionization fraction x sharply at $z \sim 10^3$. This weakens the Compton coupling to the CMB, and at $z \sim 400$ the gas temperature begins dipping slightly below the CMB temperature (*straight line*). At $z \sim 800$, a minute fraction of molecular hydrogen is formed via the H_2^+ channel before this reaction freezes out. At $z \sim 100$, density and temperature rise to their virial values. This causes a surge in the production of H_2 via the H^- channel, producing a molecular abundance close to 10^{-3}, and this in turn causes rapid cooling. From this point on, the curves in the figure are of course irrelevant, since the density will rise, causing even more rapid cooling and a

[3] Our derivation also neglected entropy generation due to the thermalization of bulk kinetic energy. When an object virializes, the infall kinetic energy of the gas is thermalized in a virialization shock. Thus some entropy is generated and the pressure of the gas is higher (typically by a factor of 1–2) than predicted by the adiabatic compression. In any event, this entropy generation would only decrease the above 6/5 by a factor of order unity and would not change the results substantially.

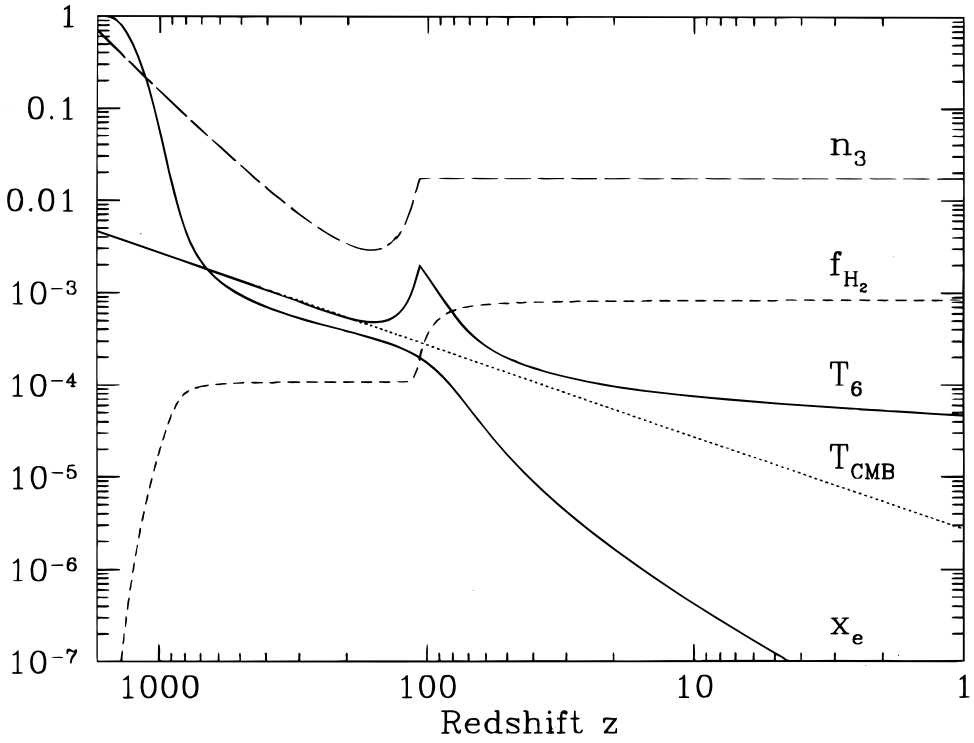

FIG. 3.—Lump evolution. The time evolution of gas in a lump is shown for $z_{vir} = 100$, $T_{vir} = 1000$ K, $h = 0.5$, $\Omega = 1$, and $\Omega_b = 0.06$. From top to bottom, on the right side, the curves show the number density n in units of 10^3 cm^{-3} the molecular fraction f, the temperature T in units of 10^6 K, the CMB temperature in the same units, and the ionization fraction x.

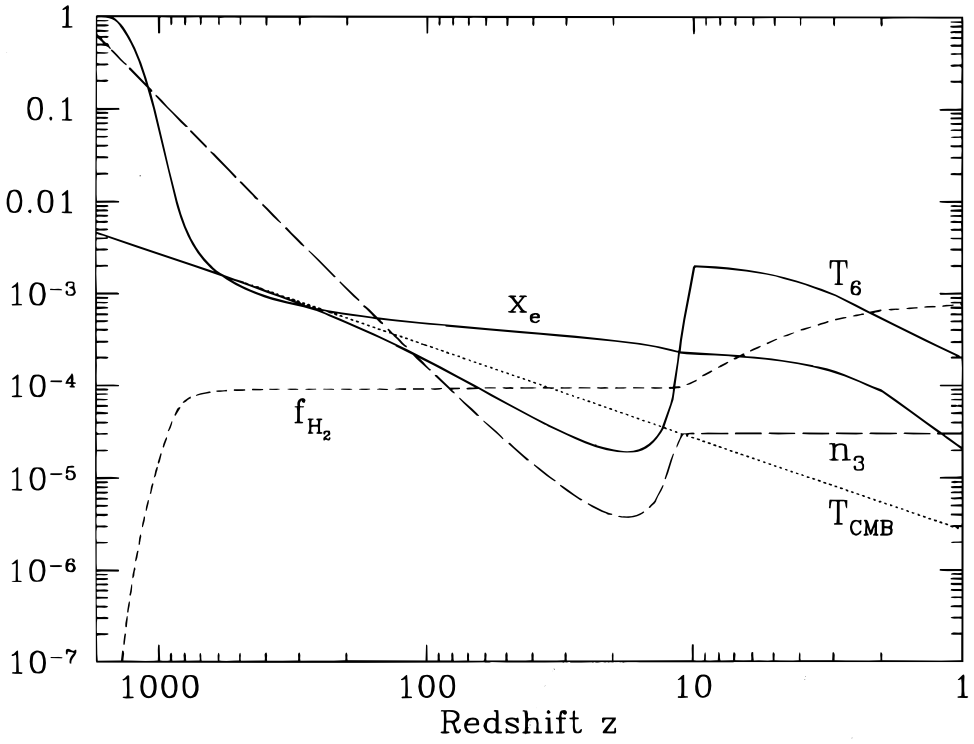

FIG. 4.—Lump evolution. Same as previous figure, except that $z_{vir} = 10$.

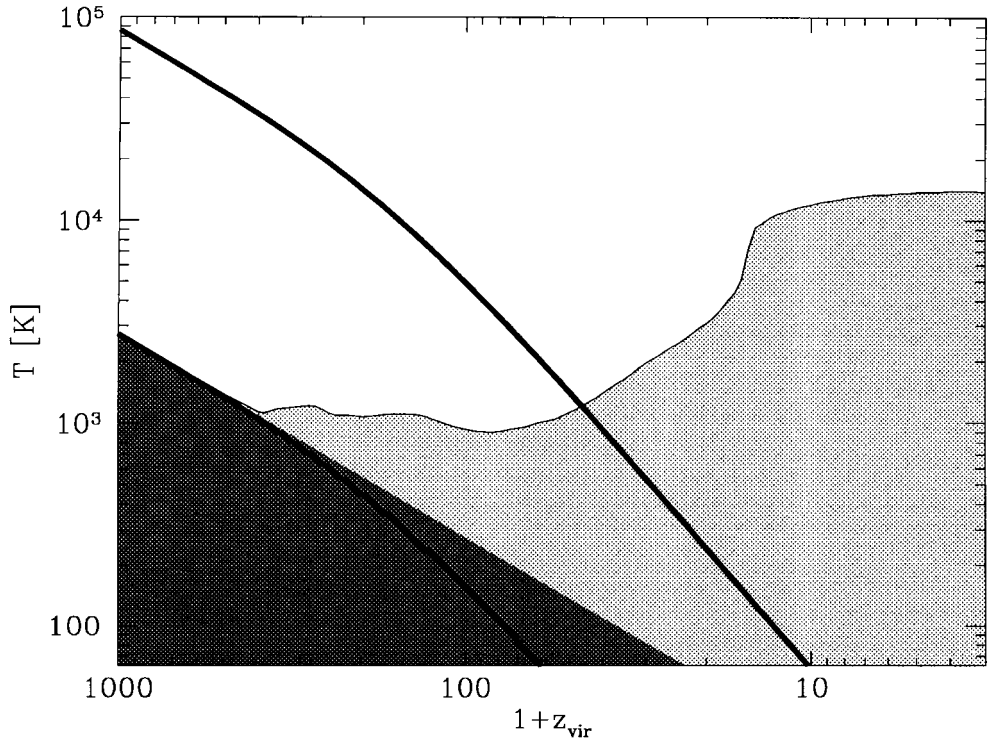

FIG. 5.—The minimum virial temperature needed to collapse. The minimum T_{vir} for which collapse succeeds is plotted as a function of virialization redshift for standard CDM ($\Omega = 1$, $\Omega_b = 0.06$, $h = 0.5$). Only lumps whose parameters (z_{vir}, T_{vir}) lie above the shaded area can collapse and form luminous objects. The dark shaded region is that in which no radiative cooling mechanism whatsoever could help collapse, since T_{vir} would be lower than the CMB temperature. The solid curves show the temperature evolution of the uniform IGM and $(18\pi^2)^{2/3}$ times this value, so above the upper line, gas can attain the virial overdensity without problems with pressure support.

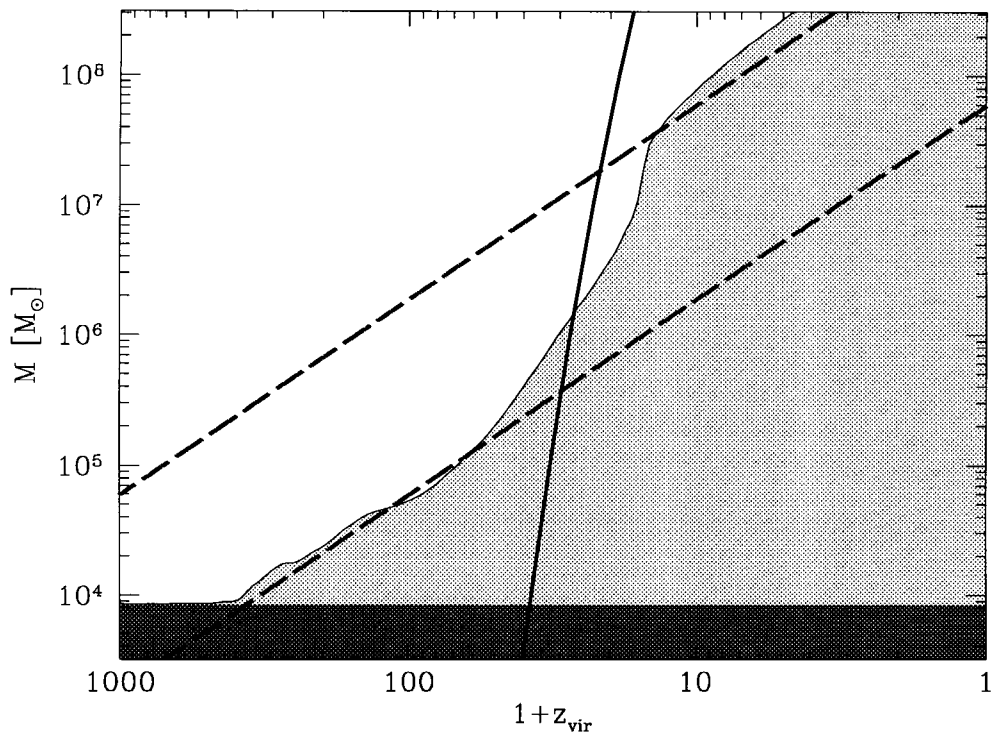

FIG. 6.—The minimum mass needed to collapse. The function $M_c(z_{vir})$ is plotted as a function of virialization redshift for standard CDM ($\Omega = 1$, $\Omega_b = 0.06$, $h = 0.5$). Only lumps whose parameters (z_{vir}, M) lie above the shaded area can collapse and form luminous objects. The dashed straight lines corresponding to $T_{vir} = 10^4$ K and $T_{vir} = 10^3$ K are shown for comparison (dashed). The dark shaded region is that in which no radiative cooling mechanism whatsoever could help collapse, since T_{vir} would be lower than the CMB temperature. The solid line corresponds to 3 σ peaks in standard CDM, normalized to $\sigma_8 = 0.7$, so such objects with baryonic mass $\Omega_b \times 2 \times 10^6\ M_\odot \sim 10^5\ M_\odot$ can form at $z = 30$.

density profile that must ultimately be modeled with a full three-dimensional hydrodynamics simulation.

The evolution of a less successful lump is shown in Figure 4, with $z_{\rm vir} = 10$. Here even the molecules produced by the H^- channel around $z \sim 100$ are too few to cause significant cooling. The molecules produced in the third wave of formation, at $z \sim z_{\rm vir}$, are unable to cool the cloud substantially simply because the density (and thus the cooling rate) has become too low (Fig. 4).

5.1. *The Collapse Criterion*

We now give our operational definition of failure to collapse. After the lump has virialized, we keep the density constant at $\rho_{\rm vir}$ and continue to integrate the equations for the time evolution of temperature, ionization fraction, and molecule abundance. Loosely speaking, we consider the cloud a failure if its temperature has not dropped substantially within a Hubble time, which roughly corresponds to the redshift dropping by a factor $2^{2/3}$. We define failure to mean that

$$T(\eta z) \geq \eta T(z)\,, \tag{37}$$

and choose $\eta = 0.75$. We do not want to choose η too small, since then even clouds that merely "loiter" for a while and suddenly cool at a substantially lower redshift (when molecule formation suddenly becomes effective) will be counted as successful.

It should be noted that Compton cooling alone is useless for making early structures. If it is able to cool the cloud substantially, the resulting contraction will drive up the recombination rate (since the CMB temperature is very much less than 10^4 K), virtually all free electrons will disappear, and Compton cooling will cease. Thus Compton cooling is self-destructive. Molecular cooling of course does not suffer from this problem once the H_2 has been produced, and can make runaway contraction proceed over many orders of magnitude. The same goes for hydrogen line cooling: although it requires free electrons, the latter will be produced collisionally at the high temperatures $\sim 10^4$ K where line cooling is effective.

To ensure that our minimum mass is that above which runaway collapse (and thus possible formation of luminous objects) can occur, we thus ignore Compton cooling when $z < z_{\rm vir}$.

5.2. *The "Shooting" Scheme*

For each virialization redshift $z_{\rm vir}$, there will clearly be some critical temperature $T_{\rm vir}$ such that clouds with $T > T_{\rm vir}$ will collapse and clouds with $T < T_{\rm vir}$ will fail. We find this critical value by a "shooting" scheme: we run the code for a very high and a very low virial temperature, then again for the average of the two temperatures, then use the interval halving method to recursively home in on the critical value $T_{\rm vir}$. This is quite feasible numerically, since each individual evolution run takes merely a few seconds on a workstation. The results are shown in Figures 5 and 6, where the shaded parts of parameter space correspond to clouds that fail to collapse.

6. DISCUSSION

Earlier work on H_2 formation in the early universe has focused on photodissociation and subsequent suppression of H_2 cooling near the first structures to form, which are a likely source of ionizing photons at high redshift (Silk 1985; Efstathiou 1992). Conversely, Haiman, Rees, & Loeb (1996a) find that at low redshift the ionizing background radiation field from the first collapsing systems may actually stimulate H_2 formation and cooling in primordial clouds. We have shown that even without ionizing radiation, enough electrons survive from the recombination epoch, even in overdense collapsing regions, for H_2 formation and cooling to be significant. Indeed, we have found that in the context of a standard CDM model, H_2 formation triggers cooling in virialized clouds and allows early formation of low-mass objects.

Typical initial conditions for the first bound objects to form (from 3 σ peaks) at $z \sim 30$ are found to be $f_{H_2} \sim 10^{-3}$, $n_{\rm H} \sim 10^2$ cm^{-3}. Clouds of baryonic mass $\sim 10^5\, M_\odot$ can be virialized at this redshift, with ensuing runaway H_2 cooling. The abundance of such objects is readily estimated by combining the Press-Schechter (Press & Schechter 1974) formalism with the accurate derivation of the small-scale transfer function given by Hu & Sugiyama (1995). The impact of these first objects depends strongly on unknown quantities such as their star formation initial mass function (IMF). The most important issue is whether they were able to emit enough ionizing radiation to reionize the universe or not. Below we will argue that they might have left observable imprints in both cases.

6.1. *If UV Emission Is Substantial ...*

Let us first consider the former case, where UV emission is substantial. Our population of condensed baryonic clouds could either undergo star formation or form massive black holes. If the former fate awaits these clouds, it is plausible to believe, by analogy with our knowledge of the most metal-poor Galactic stars, that a wide range of stellar masses is generated. In either case, a substantial production of ionizing photons is likely. In the former case, heavy elements will also be synthesized. This would give a possible source for the heavy elements found at $z = 2$–4 in Lyman-alpha forest clouds, the most primitive objects in the universe, that amount to $\sim 0.3\%$ of the solar abundances. The IGM will be reheated at $z \gtrsim 10$, thereby suppressing the formation of dwarf galaxies until a much later epoch, as argued by Blanchard et al. (1992). The low-luminosity tail of the luminosity function of faint blue galaxies is indeed inferred to steepen with lookback time, as interpreted in models of faint galaxy number counts (Treyer & Silk 1994), consistent with recent ($z \sim 1$) formation.

In addition, optical depths of at least a few percent (Tegmark & Silk 1995) to electron scattering in the IGM are inevitable if reionization occurs when the first generation of objects condenses. This would lead to noteworthy implications for satellite proposals to measure the CMB anisotropy C_l's to a precision of a percent or so. Scattering at this level would reduce the height of the acoustic peaks, which in the absence of early reionization are primarily sensitive to the baryon density.

6.2. *... and if It Is Not*

Let us now consider the latter case, where the initial UV emission is negligible. Even if star formation is successful, there are at least three possible things that could prevent substantial UV emission:

1. The IMF could be so steep that almost no OB stars are formed.

TABLE 1

REACTION RATES USED

Reaction	Rate k ($cm^3\ s^{-1}$)	Reference
$H^+ + e^- \mapsto H + h\nu$	$k_1 \approx 1.88 \times 10^{-10} T^{-0.64}$	Hutchins 1976
$H + e^- \mapsto H^- + h\nu$	$k_2 \approx 1.83 \times 10^{-18} T^{0.88}$	Hutchins 1976
$H^- + H \mapsto H_2 + e^-$	$k_3 \approx 1.3 \times 10^{-9}$	Hirasawa 1969
$H^+ + H \mapsto H_2^+ + h\nu$	$k_5 \approx 1.85 \times 10^{-23} T^{1.8}$	Shapiro & Kang 1987
$H_2^+ + H \mapsto H_2 + H^+$	$k_6 \approx 6.4 \times 10^{-10}$	Karpas et al. 1979
$H^- + h\nu \mapsto H + e^-$	$k_4 \approx 0.114 T_\gamma^{2.13} e^{-8650/T_\gamma}$	Appendix
$H_2^+ + h\nu \mapsto H + H^+$	$k_7 \approx 6.36 \times 10^5 e^{-71600/T_\gamma}$	Appendix
$e^- + h\nu \mapsto e^- + h\nu$	$k_8 \approx 4.91 \times 10^{-22} T_\gamma^4$	

NOTE.—Rates in the first five rows are in $cm^3\ s^{-1}$; those in the last three rows are in s^{-1}. All temperatures are in kelvins.

2. The bulk of the UV radiation could be absorbed locally, so that most of the radiation leaving the cloud is degraded below the Lyman limit.

3. Since the clump would be quite loosely bound, with a virial temperature $\ll 10^4$ K, the first few massive stars might photoionize the entire cloud, blow out the gas, and thus prevent the bulk of the baryons from forming stars.

If any of these caveats apply, then a much larger fraction (i.e., not just 3 σ peaks) of the baryons would have time to form stars before global reionization finally raised the Jeans mass to above 10^4K and terminated this production of small objects. This turnoff might not occur until $z \sim 5$–10, which could leave as much as 50% of the baryons in condensed MACHO-like objects. For a low-density CDM cosmology with $\Omega \sim 0.3$ and a nucleosynthesis-favored baryon fraction $\Omega_b \sim 0.06$, this would imply that about 10% of our Galactic halo would consist of MACHOs.

The authors would like to thank Martin Haehnelt, Uffe Hellsten, Avi Loeb, and Ned Wright for useful suggestions. This work has been partially supported by European Union contract CHRX-CT93-0120 and Deutsche Forschungsgemeinschaft grant SFB-375.

APPENDIX

In this appendix we provide fits to the CMB photodissociation rates of H^- and H_2^+.

The cross section for photodissociation of H^- of Wishart (1979) is well fitted by the expression

$$\sigma \approx 3.486 \times 10^{-16}\ \mathrm{cm}^2 \times \frac{(x-1)^{3/2}}{x^{3.11}}\,, \tag{38}$$

where $x \equiv h\nu/0.74\mathrm{eV}$. The cross section for photodissociation of H_2^+ from the ground state has been accurately calculated by Stancil (1994), and we find that these numerical results are well fitted by the expression

$$\sigma \approx 7.401 \times 10^{-18}\ \mathrm{cm}^2 \times 10^{-x^2 - 0.0302x^3 - 0.0158x^4}\,, \tag{39}$$

where $x \equiv 2.762 \ln(h\nu/11.05\mathrm{eV})$. The cross section vanishes below the binding energy $h\nu = 2.65$ eV. To obtain the desired dissociation rates k, we simply integrate the above cross sections against a Planck spectrum:

$$k = \frac{8\pi}{c^2} \int_0^\infty \frac{\nu^2 \sigma(\nu) d\nu}{e^{h\nu/kT_\gamma} - 1}\,, \tag{40}$$

and fit the numerical results by the simple expressions given in Table 1. The rate k_4 is accurate to within 10% for the redshift range $40 < z < 2000$, and k_7 is correct to within 50% for $150 < z < 1500$.

REFERENCES

Abel, T. 1995, Ph.D. thesis, Univ. Regensburg
Abel, T., Anninos, P., Norman, M. L., & Zhang, Y. 1996a, in preparation
Abel, T., Anninos, P., Zhang, Y., & Norman, M. L. 1996b, New Astron., submitted
Anninos, P., Zhang, Y., Abel, T., & Norman, M. L. 1996, New Astron., submitted
Bardeen, J. M., Bond, J. R., Kaiser, N., & Szalay, A. S. 1986, ApJ, 304, 15
Binney, J. 1977, ApJ, 215, 483
Blanchard, A., Valls-Gabaud, D., & Mamon, G. A. 1992, A&A, 264, 365
Bond, J. R., & Szalay, A. S. 1983, ApJ, 274, 443
Cen, R., Ostriker, J. P., & Peebles, P. J. E. 1993, ApJ, 415, 423
Cole, S., Aragon-Salamanca, A., Frenk, C. S., Navarro, J. F., & Zepf, S. E. 1994, MNRAS, 271, 781
Couchman, H. M. P. 1985, MNRAS, 214, 137
Couchman, H. M. P., & Rees, M. J. 1986, MNRAS, 221, 53
Dalgarno, A., & McCray, R. A. 1972, ARA&A, 10, 375
de Araujo, J. C. N., & Opher, R. 1988, MNRAS, 231, 923
de Araujo, J. C. N., & Opher, R. 1989, MNRAS, 239, 371
———. 1991, ApJ, 379, 461
Efstathiou, G. 1992, MNRAS, 256, 43P
Fukugita, M., & Kawasaki, M. 1991, MNRAS, 269, 563
Gnedin, N. Y., & Ostriker, J. P. 1992, ApJ, 400, 1
Gunn, J. E., & Peterson, B. A. 1965, ApJ, 142, 1633
Haiman, Z., Rees, M. & Loeb, A. 1996a, ApJ, 467, 522
Haiman, Z., Thoul, A. A., & Loeb, A. 1996b, ApJ, 464, 523 (HTL96)
Hirasawa, T. 1969, Prog. Theor. Phys., 42, 523
Hollenbach, D., & McKee, C. F. 1979, ApJS, 41, 555
Hu, W., Scott, D., & Silk, J. 1994, Phys. Rev. D, 49, 648
Hu, W., & Sugiyama, N. 1995, preprint, astro-ph/9510117
Hutchins, J. B. 1976, ApJ, 205, 103
Karpas, Z., Anicich, V., & Huntress. 1979, J. Chem. Phys., 70, 2877
Kauffmann, G, White, S. D. M., & Guiderdoni, B. 1993, MNRAS, 264, 201
Lepp, S., & Shull, J. M. 1983, ApJ, 270, 578
Liddle, A. R., & Lyth, D. H. 1995, MNRAS, 273, 1177

Loeb, A. 1996, private communication
Mather, J. C., et al. 1994, ApJ, 420, 439
Peebles, P. J. E. 1987, ApJ, 315, L73
———. 1993, Principles of Physical Cosmology (Princeton: Princeton Univ. Press)
Press, W. H., & Schechter, P. 1974, ApJ, 187, 425
Puy, D., et al. 1993, A&A, 267, 337
Puy, D., & Signore, M. 1996, A&A, 305, 371
Rees, M. J., & Ostriker, J. P. 1977, MNRAS, 179, 541
Shapiro, P. R., & Kang, H. 1987, ApJ, 318, 32
Silk, J. 1977, ApJ, 211, 638
———. 1985, ApJ, 297, 1
Smoot, G. F., et al. 1992, ApJ, 396, L1
Stancil, P. C. 1994, ApJ, 430, 360
Steidel, C. C., & Sargent, W. L. W. 1987, ApJ, 318, L11
Subrahmanyan, R., et al. 1993, MNRAS, 263, 416
Tegmark, M. 1994, Ph.D. thesis, Univ. California Berkeley
Tegmark, M., & Silk, J. 1994, ApJ, 423, 529
———. 1995, ApJ, 441, 458
Tegmark, M., Silk, J., & Blanchard, A. 1994, ApJ, 420, 484; erratum 434, 395
Treyer, M., & Silk, J. 1994, ApJ, 436, L143
Vishniac, E. 1987, ApJ, 322, 597
Webb, J. K., Barcons, X., Carswell, R. F., & Parnell, H. C. 1992, MNRAS, 255, 319
White, S. D. M., & Rees, M. J. 1978, MNRAS, 183, 341
Wishart, A. W. 1979, MNRAS, 187, 59P